Fast 3D inversion of "total field" resistive limit TEM data

Peter K. Fullagar*
Fullagar Geophysics Pty Ltd
512B-409 Granville Street
Vancouver, B.C. V6C 1T2
Canada
peter@fullagargeophysics.com

Dennis Woods
Discovery International Geophysics Inc
14342 Greencrest Drive
Surrey, B.C. V4P 1M1
Canada
dennis.woods@discogeo.com

SUMMARY

Rapid interpretation of transient electromagnetic (TEM) data sets is highly desirable for timely decision-making in exploration. However, full solution 3D inversion of TEM data sets is often impractically slow. Therefore, a fast approximate 3D TEM inversion scheme has been developed for time-integrated (resistive limit) data. The resistive limits are amenable to linear 3D magnetic inversion, which is up to 100 times faster than "rigorous" 3D TEM inversion. The resistive limit inversion scheme is suitable for airborne, ground, and downhole TEM, both dB/dt and B-field. Its efficacy is illustrated here via application to a heli-borne sub-audio magnetic (HeliSAM) data set recorded over the Lalor Zn-Cu-Au VMS deposit in Manitoba, Canada. The response from the deposit is clear in the "total field" EM (TFEM) data even though the mineralisation is very deep, extending from depth 575m to over 1100m. A three-stage inversion of resistive limits derived from the TFEM rapidly defined a 3D conductor below the uppermost pyrite-sphalerite lenses, enclosing a volume containing mainly pyrrhotite-chalcopyrite stringer sulphides. Total inversion time was less than one minute on a notebook PC.

Key words: electromagnetic, time domain, resistive limit, total field, SAM, inversion, VMS, Lalor deposit.

INTRODUCTION

Rapid interpretation of TEM data sets is highly desirable for timely decision-making in exploration. Conductivity-depth imaging (CDI), 1D inversion, and conductive plate modelling are convenient and fast, but have limitations in geologically complex environments. 3D TEM modelling and inversion programs providing full solutions to Maxwell's Equations have been developed in recent years, e.g. at University of British Columbia (Oldenburg et al, 2013) and University of Utah (Cox et al, 2012). Although the technical advances are impressive, inverting TEM surveys is often impractically slow on current day PCs, even operating in clusters. While "exact" 3D inversion is technically appealing, it is arguable whether the computational effort is always warranted, e.g. if the objective is regional reconnaissance rather than drill targeting. Moreover, the line spacing for TEM surveys is often such that the coverage is quasi-2D rather than truly 3D, also weakening the case for rigorous 3D inversion. Therefore, for reasons of both speed and practicality, a fast approximate 3D TEM inversion algorithm has been developed (Schaa & Fullagar, 2010; Fullagar & Schaa, 2014) to complement 1D and plate modelling options. The algorithm is suitable for airborne, downhole, and ground dB/dt or B-field data. Full solution 3D TEM software can be employed to refine the interpretation of potential drill targets subsequently, if required.

The algorithm, VPem3D, exploits the concept of magnetic moments (Smith & Lee, 2001, 2002). For step-current shut-off, the first order TEM moment, or resistive limit, response $\vec{M}$ is defined as

$$\vec{M} = \int_0^\infty \vec{B}(t)dt \tag{1}$$

where **B** is the magnetic flux density. In the resistive limit the induced EM response produced by a compact conductor is a magnetic dipole. The electromagnetic interaction between conductors can be ignored at late time, so the resistive limit response can be calculated as the superposition of magnetic dipoles. In effect, therefore, the integration (1) converts the 3D TEM inversion problem into a 3D magnetic inversion problem, amenable to much more rapid solution.

Time-integration transforms each TEM decay into a single value; this substantially reduces the volume of data, which delivers a further benefit in terms of inversion speed, but the time evolution of the data is lost. Three strategies are employed to compensate for that loss of information: (i) imposition of geological constraints or adoption of a geologically-based starting model, if available; (ii) construction of a data-based starting model via 3D interpolation of conductivity-depth imaging (CDI) sections or 1D inversion models; and (iii) conditioning of the solution, either by performing compact body inversion (described below) or by imposing weights. Two forms of weighting are offered: depth weighting (e.g. Li & Oldenburg, 1996), to penalise changes near-surface, and conductivity weighting (Schaa, 2010), to focus changes within conductive zones.

The fast 3D inversion scheme is illustrated below via application to HeliSAM data recorded over the Lalor VMS deposit in Canada. The SAM method was developed for simultaneously mapping the magnetic and electrical characteristics of the Earth (Cattach et al, 1993). A total field magnetometer sensor is deployed to acquire high definition data in the vicinity of a grounded dipole or closed loop transmitter. For grounded dipoles, total field magnetometric conductivity (TFMMC) data is recorded during the on-time, while the off-time decays may define either total field EM (TFEM) responses or total field magnetometric induced polarisation (TFMMIP) responses, or a combination of the two. Conventional static total magnetic intensity (TMI) data is also recorded. Data are recorded

continuously, yielding high resolution multi-parameter profiles with station intervals of just a few metres. The active source B-fields are much smaller than the geomagnetic field, so the transient B-field component parallel to the Earth's field is measured. Any component of the secondary B-field can then be recovered via potential fields processing.

At Lalor, the HeliSAM survey defined a clear TFEM response from the VMS mineralisation, notwithstanding its great depth (over 575m). Although the geology is well known, the inversion was treated as a greenfields exploration exercise and no geological constraints were imposed. A three-stage inversion of resistive limits derived from the TFEM rapidly defined a conductive zone below the uppermost pyrite-sphalerite lenses, enclosing a volume containing mainly pyrrhotite-chalcopyrite stringer sulphides. Inversion time was less than one minute on a notebook PC. This first inverted model consisted of a homogeneous conductor in a zero conductivity host. The data fit was subsequently improved by allowing for a finite conductivity host, and permitting heterogeneity in both conductor and host. The final model included a relatively weak conductor in the hangingwall stratigraphy.

FAST 3D MODELLING & INVERSION ALGORITHM

The forward algorithm divides the ground into rectangular cells and assigns a "magnetisation vector" $\vec{s}$, to each cell, defined as

$$\vec{s} = \vec{B}_0 V \tau, \tag{2}$$

where V is the volume of the cell, $\vec{B}_0$, is the primary field at its centre, and τ is the time constant of the body to which the cell belongs. Thus τ plays a role closely analogous to susceptibility in conventional magnetic modelling.

The concept of time constants is meaningful for compact conductors, but does not apply to current diffusion in extensive conductors. Therefore the forward modeling scheme adds the resistive limit response from a homogeneous or layered host model to the combined "magnetic" response of the discretised model cells. At a particular receiver location (*x,y,z*), the net TEM moment is then given by

$$\vec{M}(x,y,z) = \vec{M}_0(x,y,z) + \sum_{k=1}^{K} G_k(\vec{r}_k)\cdot\tau_k \tag{3}$$

where $\mathbf{M}_0$ denotes the host or background response, K is the number of cells, and $\mathbf{G}_k$ represents the "magnetic" response of the kth cell with position vector $\mathbf{r}_k$ relative to the receiver and with time constant τ_k,. The discretised model responses are computed using conventional magnetic modelling routines, the only difference from static magnetics being the spatial variation of the primary field produced by the TEM transmitter. Analytic expressions have been derived for the background resistive limit response on and in a half-space excited by a rectangular loop on its surface (Schaa & Fullagar, 2012; Fullagar & Schaa, 2013). For layered host models excited by transmitter loops of arbitrary shape, the resistive limit above, on, or under the ground is computed in the frequency domain using a modified version of the program described by Godber & Fullagar (2012). In the frequency domain, $\vec{M}_0$ is the derivative of the impulse response in the limit of low frequency (Smith & Lee, 2002):

$$\vec{M}_0 = \lim_{\omega\to 0} i\frac{\partial}{\partial\omega}\left(\frac{d\vec{B}}{dt}(\omega)\right) \tag{4}$$

The 3D inversion algorithm was originally developed for potential fields data (Fullagar et al, 2004). The inverse problem is solved via the method of steepest descent (Schaa & Fullagar, 2010), so no matrix inversion is required. Details are provided by Schaa (2010, Chapter 5).

3D inversion of TEM is non-unique. Incorporation of geological constraints, if available, reduces the non-uniqueness (Fullagar & Pears, 2007). Integrated interpretation is achieved most naturally if inversion is performed on a geological model, with the sub-surface is divided into rock type domains. VPem3D can operate on geological models, which are both categorical and quantitative, whereas most inversion programs operate on "property only" models. Geological models permit geometry inversion, i.e. adjustment of geological boundaries (Fullagar et al, 2008), as well as property inversion. Conductivity changes during inversion can be constrained by upper and lower bounds, specific to each geological unit. In addition, the inversion can be restricted easily to selected geological units of prime interest, while other units play no part.

Strictly speaking, it follows from (2) that the inverted property is time constant rather than conductivity. However, time constant is not always meaningful and is not a petrophysical property in the normal sense. The time constant of simple bodies is proportional to conductivity, but dependent on size and shape as well (Nabighian & Macnae, 1991). The constant of proportionality is also affected by the finite time interval spanned by any measured decay; the achievable integration range in (1) is never infinite. In VPem3D, for the "linear" algorithm used here, the inverted property is estimated conductivity, σ_e, calibrated against the ideal resistive limit response from a 50m radius sphere excited by a uniform field. In practice σ_e can be regarded as proportional to conductivity, but with an unknown constant of proportionality. In exploration this somewhat elastic definition does not usually pose any serious problems because the absolute value of conductivity is generally much less important than the location and shape of the conductors.

FAST 3D INVERSION OF LALOR TFEM DATA

The Lalor Zn-Cu-Au VMS deposit lies in the eastern (Snow Lake) portion of the Paleoproterozoic Flin Flon greenstone belt in central west Manitoba. The Chisel sequence that hosts the deposit contains thin and discontinuous volcaniclastic units and intermediate to felsic flow-dome complexes. The Lalor Lake deposit is similar to other massive sulphide bodies in the Chisel sequence and lies along the same stratigraphic horizon as the Chisel Lake and Chisel North deposits. The top of the mineralised zone is close to an interpreted decollement contact with unaltered but overturned hangingwall rocks (Figure 1). The mineralisation occurs

as stacked zinc-rich massive sulphide lenses, interspersed with stringer and disseminated sulphide zones (Taylor, 2014), extending from a depth of 575m to over 1100m. The massive sulphide lenses are pyrite-dominated and tend to be less conductive than the generally deeper pyrrhotite-chalcopyrite stringer sulphide zones.

The fast 3D inversion algorithm has been applied to a HeliSAM TFEM data set recorded over Lalor in August 2014 (Parker et al, 2014). A total of 93 line km of TFEM data was acquired along NE-SW lines at a nominal line spacing of 100m. The survey layout is shown in Figure 2 in a rotated coordinate system, with local east oriented parallel to flight lines (true bearing 48°). The sensor altitude was approximately 40m and the along line sampling interval was about 5m. A 50% duty cycle square wave with peak current 20A was transmitted into a single-turn loop, approximately 1.7 km square, at a frequency of 7.5 Hz. The HeliSAM TFEM data has been inverted previously by Yang & Oldenburg (2016).

Resistive limit estimates were computed by integrating the measured decays over time. The SW side of the transmitter loop followed a power line for much of its length. The power line has lightning protection, with a conductor strung between pylons and grounded at each pylon. Consequently there is a strong, early-time EM induction response from the lightning protection infrastructure. In order to minimise any distortion from this source during inversion, the first 7 channels were disregarded everywhere, and "incomplete" resistive limits were computed over the time range 3.54 to 32.71 ms.

An image of the "total field" resistive limit, RLT, in the rotated coordinate system is shown in Figure 5a. This is the resistive limit component in the direction of the geomagnetic field, which has true declination 5.25^o (local declination 47.25^o) and inclination 78.05^o at Lalor. The anomaly over the Lalor deposit is a low because the upward directed B-field response opposes the ambient field.

Model cells were 100 x 100 x 25m, draped below the topography to a depth of 2km. Conductivity was zero everywhere initially. The flight line data were gridded onto cell centres. Given the resistivities of thousands of ohm.m in unmineralised and unaltered host rocks at Lalor (DGI Geoscience) and given the great depth of the target, there is little likelihood that this data decimation (to 959 RLT values) has resulted in any significant loss of information.

Inversion proceeded in five stages:

1. Compact body inversion
2. Editing and optimisation of conductivity of homogenous compact target
3. Geometry inversion of homogeneous target
4. Heterogeneous inversion of target with uniform half-space optimisation
5. Heterogeneous inversion of host rock with uniform half-space optimisation.

A simple homogeneous conductor model was generated during the first 3 stages, using compact body and geometry inversion. Compact body inversion is an option within VPem3D which favours conductors with low volume. For any given anomaly, the compact solutions will be deeper and more conductive than solutions with greater volume. Therefore compact body inversion is well suited to VMS exploration, where the target is usually highly conductive and often fairly deep. Given that most data sets include contributions from multiple sources, producing responses with different wavelengths, it is often desirable to edit the model after compact body inversion. At Lalor the compact body conductor included a deep root with relatively low conductivity. The root was edited by simply zeroing all cells with conductivity less than 30% of the maximum value. The conductivity of the retained cells was assumed uniform; its optimal (minimum misfit) σ_e value was found to be 277 S/m.

Geometry inversion was then performed, to allow the conductor to change shape in response to the data. A 3D section view through the conductive body after compact body and geometry inversion is shown in Figure 3. The interpreted conductor lies below the uppermost pyrite-sphalerite lenses, and encloses a volume containing the more conductive pyrrhotite-chalcopyrite stringer zones. The lateral extent of the conductive volume at depth ~1060m (Figure 4) corresponds quite closely to the extent of the ore lenses (Figure 2). Thus compact body inversion followed by geometry inversion has produced a good first interpretation of the HeliSAM data, comprising a homogeneous 3D conductor in a zero conductivity host. The RMS misfit was reduced from 102.0 to 31.0 pTms/A. Total run time for stages 1 - 3 was 56s on a Dell notebook PC (2.60 GHz, 16GB RAM).

The data fit can be improved by allowing for a non-zero uniform half-space response, and permitting heterogeneity in both the conductive body and the host stratigraphy. The geomagnetic field is nearly vertical at Lalor, and the vertical resistive limit response for a fixed loop on a half-space is a bell-like anomaly centred over the loop (Schaa & Fullagar, 2012). Therefore the RLT half-space response at Lalor is a broad low centred on the transmitter loop. The half-space conductivity was optimised during the heterogeneous inversions; the optimal value was 0.41 mS/m.

Sections through the 3D conductivity model after the heterogeneous inversion runs are shown in Figure 5. Depth weighting was applied during inversion of the host rock, to penalise model changes near-surface. The heterogeneity introduced into the principal conductor is evident in Figure 5a, while much weaker conductivity variations in the host are visible in Figure 5b. A shallow conductive zone has been introduced in order to explain the intense RLT low located in the central north of the loop (Figure 5a). This conductor is interpreted to lie within the Lalor hangingwall (Figure 1), and is the correspondent of the vertical conductor attributed to a variably mineralised (pyrrhotitic?) argillite by Yang & Oldenburg (2016). The heterogeneous inversions of target and host reduced the RMS misfit from 31.0 to 21.3 pTms/A. Total run time for stages 4 - 5 on the Dell notebook PC was 113s, including 65s for the resistive limit background response calculation.

CONCLUSIONS

A program has been developed to perform fast approximate inversion of TEM in a 3D geological framework. A substantial increase in speed is achieved by exploiting the fact that compact conductors produce magnetic dipole responses in the resistive limit. Therefore integrating the TEM decays over time in effect transforms the non-linear TEM inversion problem into a quasi-linear magnetic inversion problem. The approach is suitable for inversion of airborne, ground, and downhole TEM data, both dB/dt and B-field. Run times can be reduced from hours or even days to minutes.

The trade-off for high speed is loss of information carried by the time evolution of the measured transients. Three strategies are employed to compensate: (i) imposition of geological constraints, if available; (ii) construction of a starting model from CDI sections or 1D inversion models; and (iii) conditioning of the solution, either by performing compact body inversion or by imposing weights.

The inversion algorithm described here can operate on a geological model, i.e. one capturing both lithology and conductivity. Categorical/quantitative models are a force for integration in their own right, and also offer a number of practical advantages over pure property models during inversion. In particular, they permit geometry inversion as well as property inversion. On the other hand, if little or nothing is known about the geology, "unconstrained" inversion can be performed.

The algorithm has been applied to a HeliSAM TFEM data set recorded over the Lalor VMS deposit in Manitoba. The Lalor deposit is comprised of stacked massive sulphide lenses, interspersed with stringer and disseminated sulphides, extending from a depth of 575m to over 1100m. A clear TFEM response was recorded over the deposit, notwithstanding the great depth of the mineralisation.

Compact body inversion, which favours deep and highly conductive solutions, was run first. Only the conductive top of the inverted body was retained: cells with conductivity less than 30% of the maximum value were discarded. The optimal σ_e of the edited conductor, assumed uniform, was found to be 277 S/m. Geometry inversion was then applied. The re-shaped homogeneous conductor lies below the uppermost pyrite-sphalerite massive sulphide lenses, and encloses a volume containing more conductive pyrrhotite-chalcopyrite stringer sulphides. The lateral extent of the conductive volume at a depth of about 1 km corresponds quite closely to the plan projection of the ore lenses. Thus compact body inversion followed by geometry inversion produced a good first interpretation of the HeliSAM data. Total run time was less than a minute on a notebook PC.

An improved data fit was achieved by allowing for a uniform half-space response, and permitting heterogeneity in both the target and host stratigraphy. The optimal uniform half-space conductivity was 0.41 mS/m. Depth weighting was applied during heterogeneous unit inversion of the host rock. A shallow conductive zone was introduced in order to explain the intense RLT low located in the central north of the loop. This conductor is interpreted to lie within the Lalor hangingwall stratigraphy. Total run time for these heterogeneous inversions on the notebook PC was 113s.

In conclusion, this work has demonstrated how the resistive limit TEM inversion algorithm can expedite timely and geologically acceptable initial 3D interpretation of TEM surveys. Full solution 3D TEM software can be employed to refine the interpretation of potential drill targets subsequently, if required.

ACKNOWLEDGMENTS

Our thanks to HudBay Minerals for providing access to Lalor data for this and many other studies. Scott Napier (Mira Geoscience, Vancouver) assisted with preparation of figures.

REFERENCES

Bailes, A., 2008, Geological Setting of the Lalor and Photo Lake VMS Deposits: HudBay Minerals internal report.

Cattach, M.K., Stanley, J., Lee, S.J. and Boyd, G., 1993, Sub-Audio Magnetics (SAM) high resolution technique for simultaneously mapping electrical and magnetic properties: Exploration Geophysics, 24, 387–400.

Cox, L.H., Wilson, G.A. and Zhdanov, M.S, 2012, 3D inversion of airborne electromagnetic data: Geophysics, 77, WB59-WB69.

Fullagar, P.K., Pears, G.A., Hutton, D., and Thompson, A., 2004, 3D Gravity and Aeromagnetic Inversion for MVT Lead-Zinc Exploration at Pillara, Western Australia: Exploration Geophysics, 35, 142-146.

Fullagar, P.K., and Pears, G.A., 2007, Towards geologically realistic inversion: Proceedings of Exploration '07, Fifth Decennial International Conference on Mineral Exploration, Toronto.

Fullagar, P.K., Pears, G.A., and McMonnies, B., 2008, Constrained inversion of geological surfaces - pushing the boundaries: The Leading Edge, 27, 98-105.

Fullagar, P.K., and Schaa, R., 2013, Rapid Inversion of TEM Data: AMIRA Project P1022 Final Report.

Fullagar, P.K., and Schaa, R., 2014, Fast 3D inversion of transient electromagnetic (TEM) resistive limit data: 84th Annual International Meeting, SEG, Denver, Expanded Abstracts, 1827-1831.

Godber, N.J., and Fullagar, P.K., 2012, "Unsmooth" 1D inversion of frequency domain marine controlled source EM data: ASEG Extended Abstract, 22nd International Geophysical Conference and Exhibition, Brisbane.

Li, Y., and Oldenburg, D.W., 1996, 3D inversion of magnetic data: Geophysics, 61, 394-408.

Nabighian, M.N., and Macnae, J.C., 1991, Electromagnetic Methods in Applied Geophysics: Investigations in Geophysics No. 3, Vol. 2, Society of Exploration Geophysicists, pp427-520.

Oldenburg, D.W., Haber, E., and Shekhtman, R., 2013, Three dimensional inversion of multisource time domain electromagnetic data: Geophysics, 78, E47-E57.

Parker, C., Rudd, J., Cattach, M., and Kuttai, J., 2014, The results of a HeliSAM test survey over the Lalor VMS deposit, Snow Lake, Manitoba, Canada: *in* Exploration for Deep VMS Orebodies – the HudBay Lalor Case Study, B.C. Geophysical Society, 2014 Fall Symposium Proceedings, Vancouver.

Schaa, R., 2010, Rapid Approximate Inversion of 3D Transient Electromagnetic Data: unpubl. Ph.D. thesis, University of Tasmania.

Schaa, R., and Fullagar, P. K., 2010, Rapid approximate 3D inversion of transient electromagnetic (TEM) data: 80th Annual International Meeting, SEG, Denver, Expanded Abstracts, 650-654.

Schaa, R., and Fullagar, P.K., 2012, Vertical and horizontal resistive limit formulas for a rectangular loop source on a conductive half-space: Geophysics, 77, E91-E99.

Smith, R.S., and Lee, T.J., 2001, The impulse-response moments of a conductive sphere in a uniform field – a versatile and efficient electromagnetic model: Exploration Geophysics, 32, 113-118.

Smith, R. S., and T. J. Lee, 2002, The moments of the impulse response: A new paradigm for the interpretation of transient electromagnetic data: Geophysics, 67, 1095–1103.

Taylor, C., 2014, Mine scale description of the mineralization at the Lalor deposit, Snow Lake, Manitoba, Canada: *in* Exploration for Deep VMS Orebodies – the HudBay Lalor Case Study, B.C. Geophysical Society, 2014 Fall Symposium Proceedings, Vancouver.

Yang, D., and Oldenburg, D.W., 2016, 3D inversion of total magnetic intensity data for time-domain EM at the Lalor massive sulphide deposit: Exploration Geophysics, http://dx.doi.org/10.1071/EG15070.

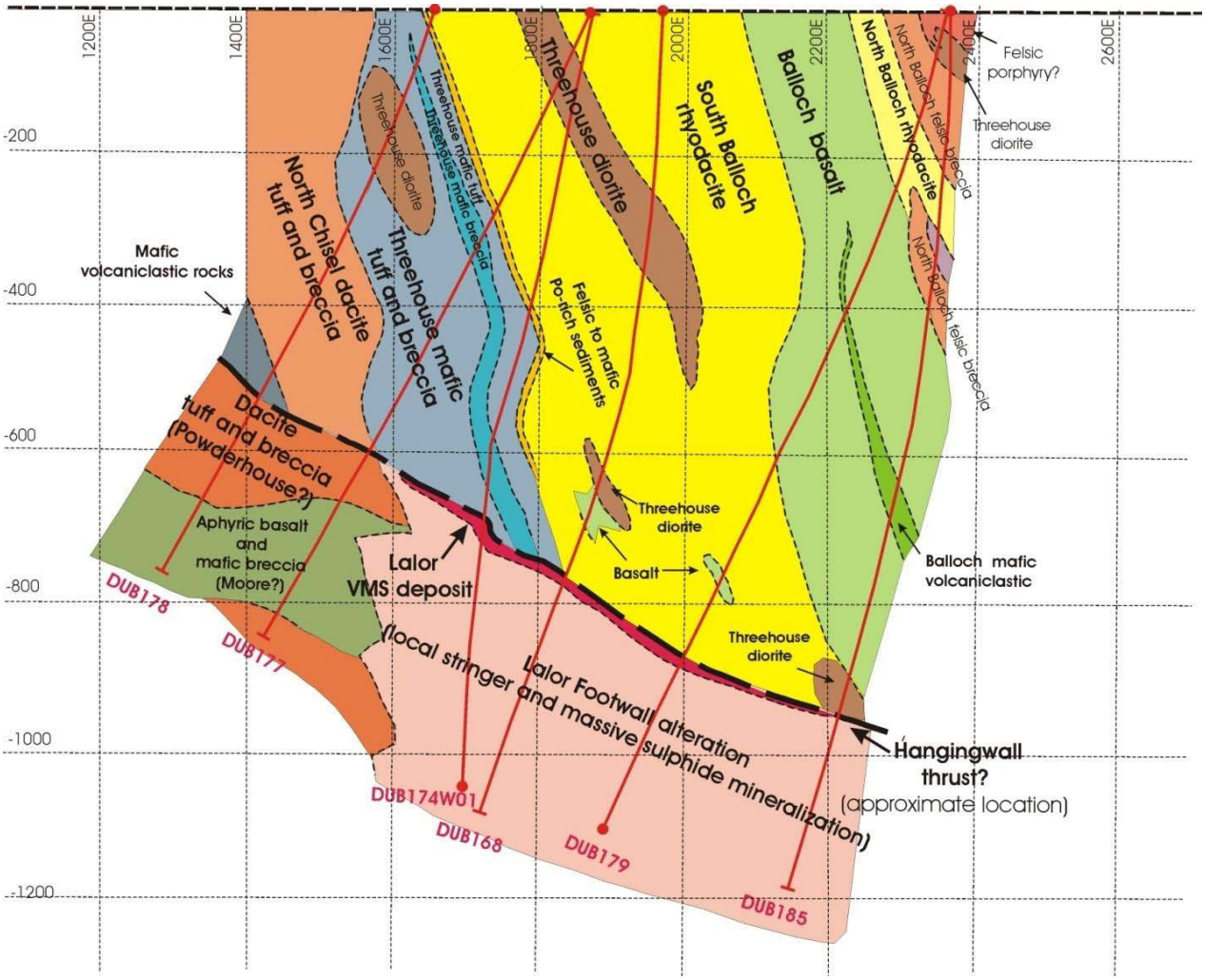

Figure 1: Simplified E-W geological section through the Lalor deposit (Bailes, 2008).

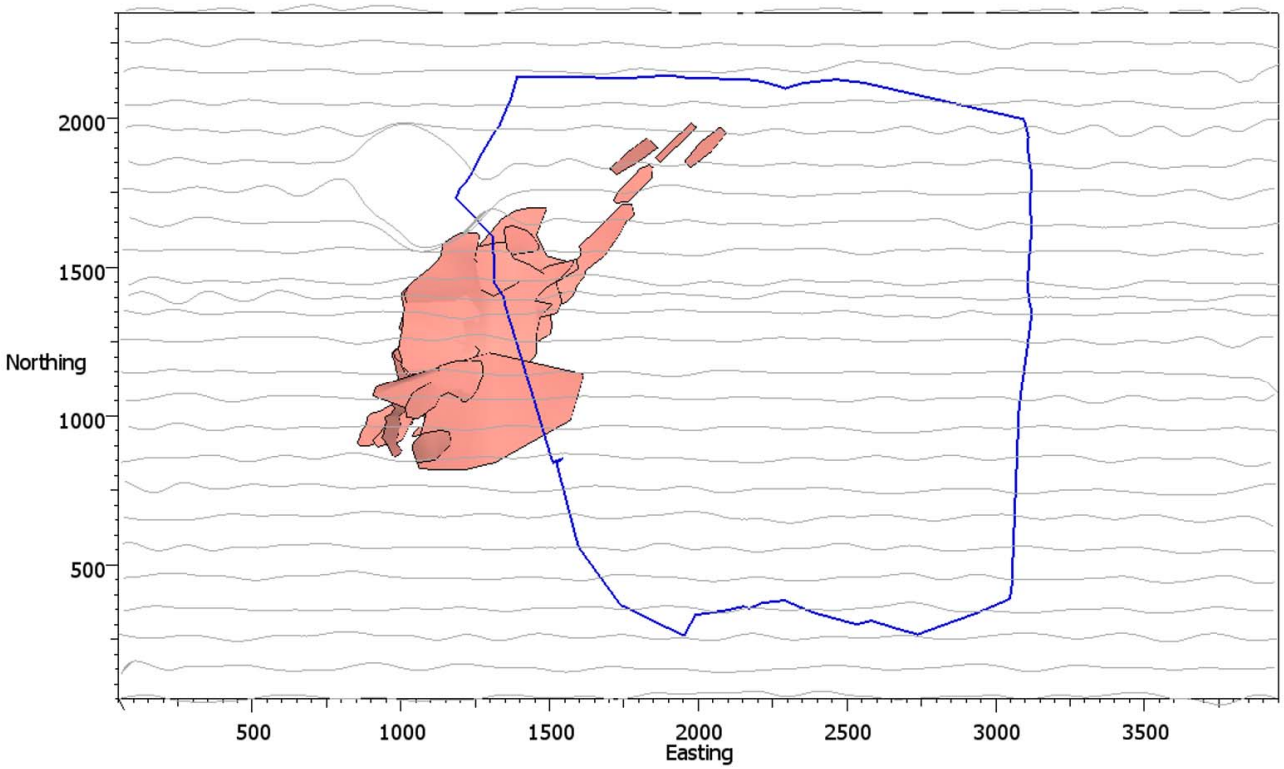

Figure 2: Lalor HeliSAM survey layout in rotated coordinates, with massive sulphide ore shells projected (pink). Local east is at true bearing 48°. Flight lines (grey) and transmitter loop (blue) superimposed.

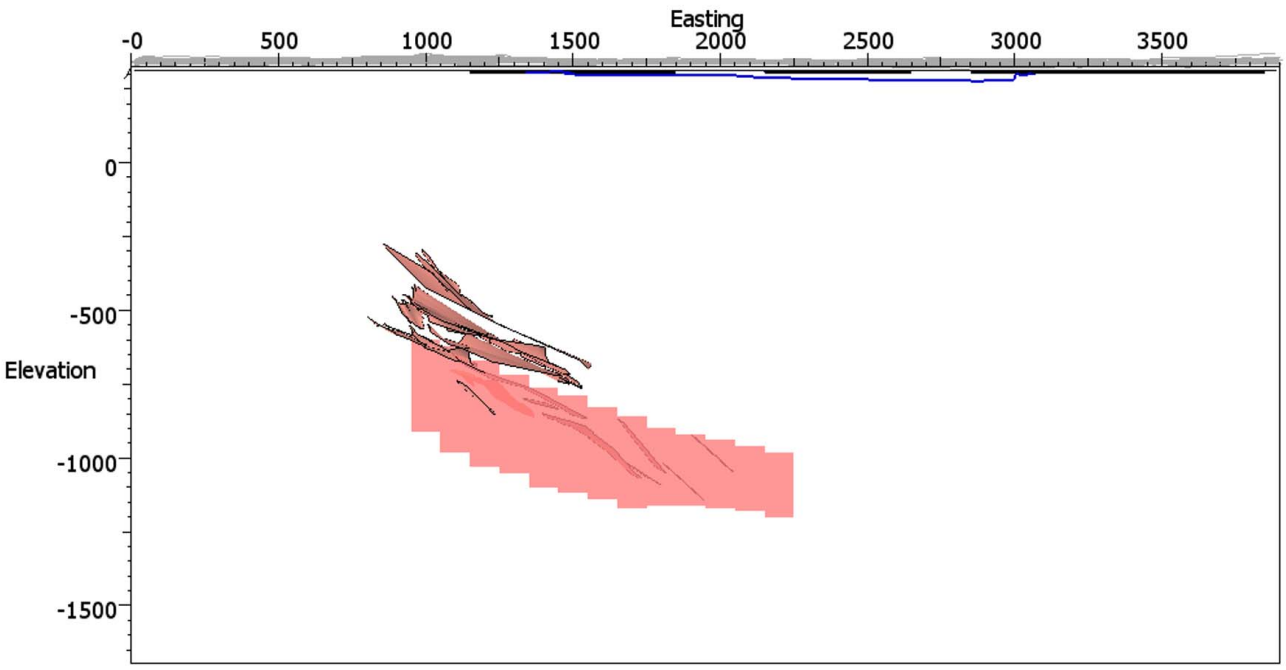

Figure 3: Inverted homogeneous conductivity model section on 1200N after compact body and geometry inversion, with massive sulphide ore shells projected. Estimated conductivity is 277 S/m inside the body, and zero elsewhere. Transmitter loop (blue) superimposed at top.

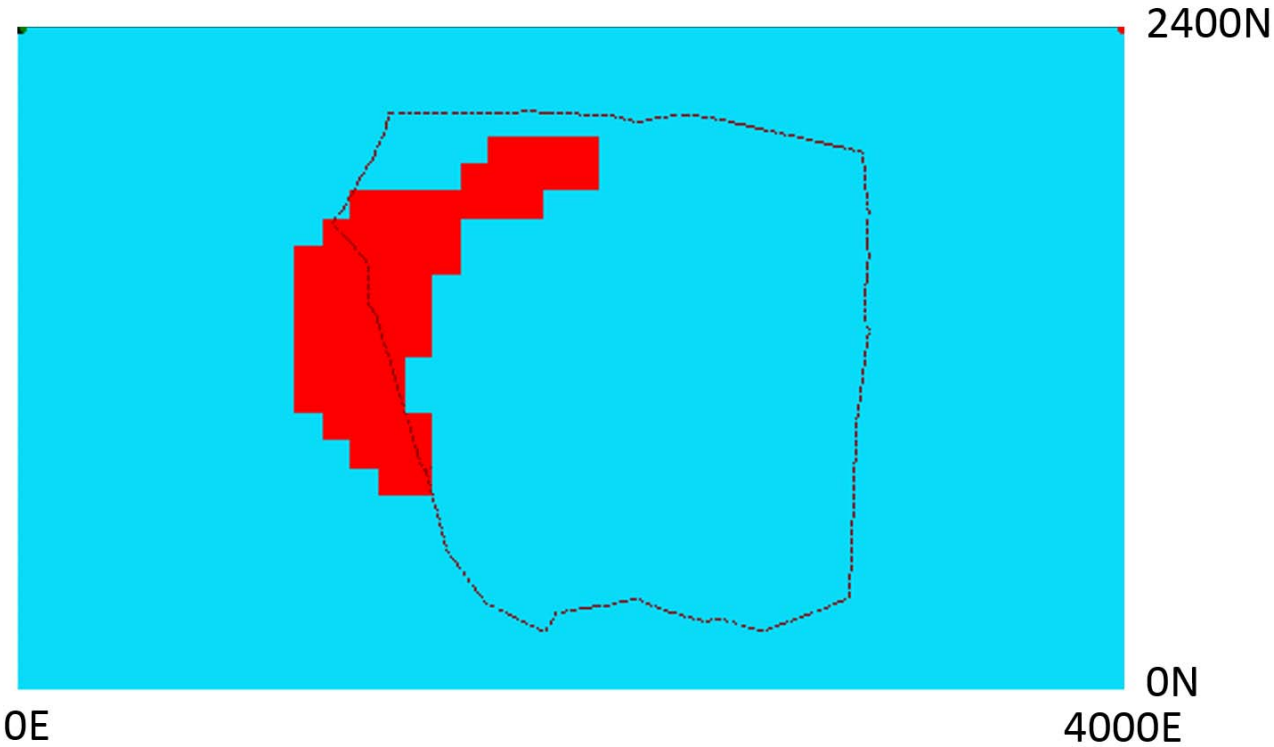

Figure 4: Horizontal slice through homogeneous conductivity model at elevation -759m (depth ~1060m) after compact body and geometry inversion. Estimated conductivity 277 S/m inside the body (red), and zero elsewhere (blue). Transmitter loop (dashed) superimposed.

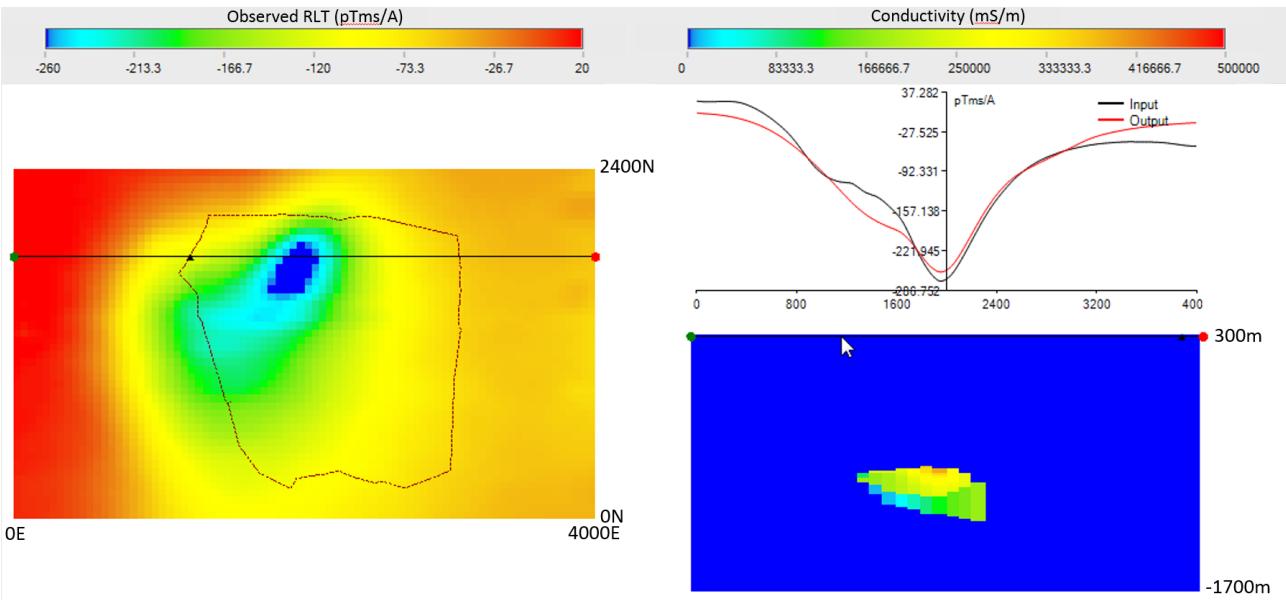

Figure 5a: Observed RLT (left) with Tx loop superimosed, and 1800N (local) section through inverted model (lower right) after heterogeneous inversion of main conductor and host. Cursor marks Tx wire. Observed (black) and calculated (red) RLT plotted at upper right. Colour bar adjusted for range 0 – 500 S/m, to display estimated conductivity variation within the main conductive zone.

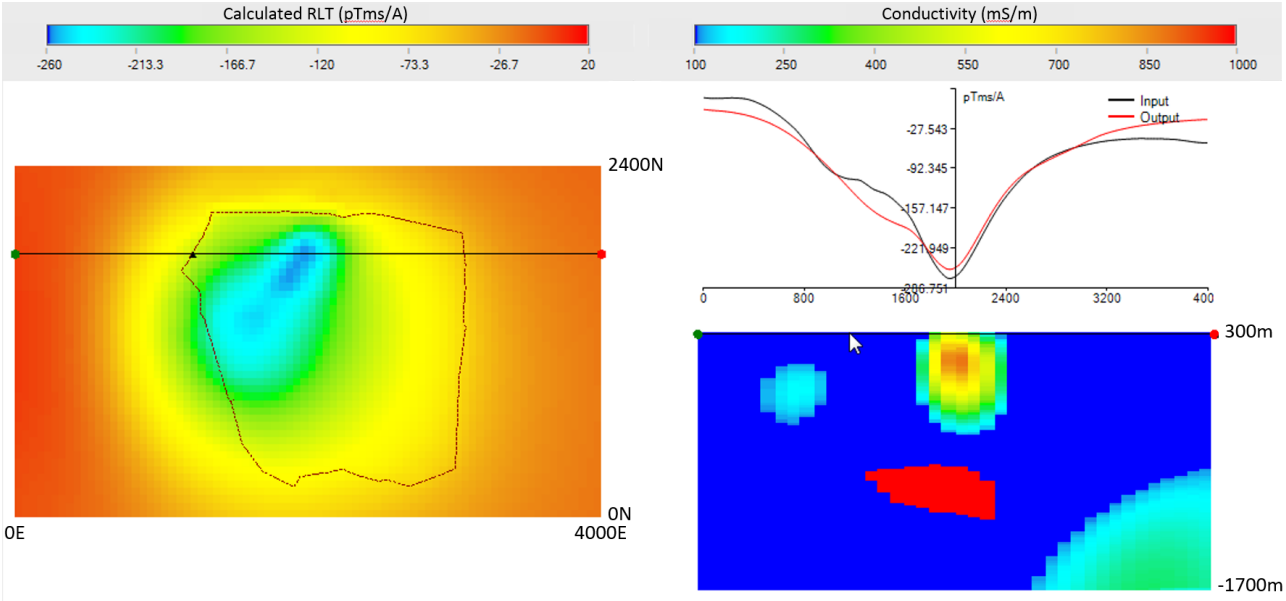

Figure 5b: Calculated RLT (left) with Tx loop superimosed, and 1800N (local) section through inverted model (lower right) after heterogeneous inversion of main conductor and host. Cursor marks Tx wire. Observed (black) and calculated (red) RLT plotted at upper right. Colour bar adjusted for range 0.1 to 1 S/m, to reveal conductivity variations within the host rocks.